Given the effect of continuity of dosing and nonlinearity of elimination, pharmacokinetic evaluations should accompany new dosing strategies for this drug.

Acknowledgments

The authors thank Pam McGill, Xiangjun Cai, and May Chung for their technical assistance; all patients and their families for their participation; and participating clinicians and research staff, including Deqing Pei.

This work was supported by National Institutes of Health, National Cancer Institute (CA142665, CA21765), investigator-initiated research funding from Servier, and the American Lebanese Syrian Associated Charities (ALSAC).

Authorship

Contribution: Y.L., J.C.P., and M.V.R. developed the pharmacokinetic model, analyzed and interpreted the data, and wrote the manuscript; S.J., C.-H.P., H.I., C.C., M.V.R., and W.E.E. developed the protocol; S.J., C.-H.P., and H.I. recruited patients and interpreted the data; C.C. and W.Y. analyzed the data; and J.J.Y., S.E.K., and W.E.E. interpreted the data.

Conflict-of-interest disclosure: M.V.R., H.I., C.-H.P., and St. Jude Children's Research Hospital receive investigator-initiated research funding from Servier Pharmaceuticals. C.-H.P. also received an honorarium from Servier Pharmaceuticals. The remaining authors declare no competing financial interests.

ORCID profiles: W.Y., 0000-0002-7305-5649; S.E.K., 0000-0001-8113-8180; C.-H.P., 0000-0003-0303-5658; M.V.R., 0000-0002-3720-9591.

Correspondence: Mary V. Relling, St. Jude Children's Research Hospital, 262 Danny Thomas Pl, Room I5112, Memphis, TN 38105; e-mail: mary.relling@stjude.org.

Footnotes

Submitted 21 April 2020; accepted 23 July 2020; prepublished online on *Blood* First Edition 4 August 2020.

The online version of this article contains a data supplement.

REFERENCES

1. Armstrong JK, Hempel G, Koling S, et al. Antibody against poly(ethylene glycol) adversely affects PEG-asparaginase therapy in acute lymphoblastic leukemia patients. *Cancer*. 2007;110(1):103-111.
2. Liu Y, Smith CA, Panetta JC, et al. Antibodies predict pegaspargase allergic reactions and failure of rechallenge. *J Clin Oncol*. 2019;37(23):2051-2061.
3. Jeha S, Pei D, Choi J, et al. Improved CNS control of childhood acute lymphoblastic leukemia without cranial irradiation: St Jude Total Therapy Study 16. *J Clin Oncol*. 2019;37(35):3377-3391.
4. Kloos RQH, Pieters R, Jumelet FMV, de Groot-Kruseman HA, van den Bos C, van der Sluis IM. Individualized asparaginase dosing in childhood acute lymphoblastic leukemia. *J Clin Oncol*. 2020;38(7):715-724.
5. Liu Y, Fernandez CA, Smith C, et al. Genome-wide study links PNPLA3 variant with elevated hepatic transaminase after acute lymphoblastic leukemia therapy. *Clin Pharmacol Ther*. 2017;102(1):131-140.
6. Ishida T, Kiwada H. Accelerated blood clearance (ABC) phenomenon upon repeated injection of PEGylated liposomes. *Int J Pharm*. 2008;354(1-2):56-62.
7. Abu Lila AS, Kiwada H, Ishida T. The accelerated blood clearance (ABC) phenomenon: clinical challenge and approaches to manage. *J Control Release*. 2013;172(1):38-47.
8. Müller HJ, Löning L, Horn A, et al. Pegylated asparaginase (Oncaspar) in children with ALL: drug monitoring in reinduction according to the ALL/NHL-BFM 95 protocols. *Br J Haematol*. 2000;110(2):379-384.
9. Hempel G, Müller HJ, Lanvers-Kaminsky C, Würthwein G, Hoppe A, Boos J. A population pharmacokinetic model for pegylated-asparaginase in children. *Br J Haematol*. 2010;148(1):119-125.
10. Avramis VI, Sencer S, Periclou AP, et al. A randomized comparison of native Escherichia coli asparaginase and polyethylene glycol conjugated asparaginase for treatment of children with newly diagnosed standard-risk acute lymphoblastic leukemia: a Children's Cancer Group study. *Blood*. 2002;99(6):1986-1994.

DOI 10.1182/blood.2020006214

TO THE EDITOR:

Combinatorial treatment with menin and FLT3 inhibitors induces complete remission in AML models with activating FLT3 mutations

Hongzhi Miao,[1,*] EunGi Kim,[1,*] Dong Chen,[1,*] Trupta Purohit,[1,*] Katarzyna Kempinska,[1] James Ropa,[2] Szymon Klossowski,[1] Winifred Trotman,[3] Gwenn Danet-Desnoyers,[3] Tomasz Cierpicki,[1] and Jolanta Grembecka[1]

[1]Department of Pathology, University of Michigan, Ann Arbor, MI; [2]Department of Microbiology and Immunology, School of Medicine, Indiana University, Indianapolis, IN; and [3]Division of Hematology-Oncology, Perelman School of Medicine, University of Pennsylvania, Philadelphia, PA

The interaction between menin and the mixed lineage leukemia 1 (MLL1) protein plays an important role in aggressive acute leukemia with translocations of the *MLL1* (*KMT2A*) gene[1,2] and with mutations in the nucleophosmin (*NPM1*) gene.[3] We and others have recently shown that small-molecule inhibitors of the menin-MLL1 interaction can effectively block leukemia progression in these leukemia subtypes.[4-11] This resulted in phase 1 clinical trials with menin inhibitors, including KO-539 (registered at www.clinicaltrials.gov as #NCT04067336), in acute myeloid leukemia (AML) patients. Activating mutations in FLT3 kinase, including internal tandem duplications (FLT3-ITDs), are found in a substantial fraction of AML patients, leading to poor clinical outcomes.[12-17] Because overexpression or mutations in FLT3 often cooccur with *MLL1* translocations (16%) or *MLL1* partial tandem duplications (>50%)[15,18-21] and *NPM1* mutations (>40%),[16,22,23] we hypothesized that the antileukemic activity of menin inhibitors may synergize with

FLT3 inhibitors, paving the way for clinical translation of such drug combinations in leukemia.

To pursue combination studies, we selected our recently developed subnanomolar menin-MLL1 inhibitor MI-3454 (supplemental Figure 1A, available on the *Blood* Web site), a close structural analog of KO-539,[9] and the US Food and Drug Administration–approved FLT3 inhibitor gilteritinib or AC220 (quizartinib)[17] and performed studies in leukemia cell lines harboring both MLL fusions and FLT3-ITDs (MV4;11 and MOLM13). Indeed, simultaneous treatment with MI-3454 and gilteritinib or AC220 resulted in much stronger cell growth inhibition vs single agents in both cell lines, but not in control cells (Figure 1A-B; supplemental Figures 1B-E and 2A-E). Furthermore, combination of MI-3454 with gilteritinib resulted in much more pronounced apoptosis (60% to 80% of annexin V^+ cells), differentiation (increased levels of CD11b and CD14 and elevated expression of *MNDA*), and stronger reduction in FLT3 protein level over single agents (Figure 1C-D; supplemental Figures 3A-D and 4A-B). Next, we assessed the expression levels of *HOXA9* and *MEIS1*, the key genes implicated in *MLL1*-rearranged leukemia,[9] and found that the combination of MI-3454 and gilteritinib led to significantly stronger downregulation of *MEIS1* in both cell lines and *HOXA9* in MV4;11 cells than the single-agent treatment (Figure 1E; supplemental Figure 4C).

To explore the mechanism of the enhanced antileukemic effect of combining MI-3454 and gilteritinib, we performed RNA sequencing studies in MOLM13 cells. We observed that the combination resulted in a doubling of the number of down- and upregulated genes when compared with single agents (Figure 1F; supplemental Figure 5A; supplemental Table 1). Using k-means clustering,[24] differentially expressed genes were grouped into 5 clusters of genes with similar expression profiles (Figure 1G). Gene ontology analysis showed that clusters 1 and 4 comprised genes upregulated in all treatment conditions vs dimethyl sulfoxide control, with the combination showing a more pronounced effect than single agents, particularly in cluster 4 (Figure 1G-H). Cluster 1 comprised genes associated with leukocyte or myeloid cell activation and pathways involved in immune response, including differentiation genes *MPO*, *CEBPE*, and *MAPK14* (supplemental Tables 2 and 3). Genes in cluster 4 also suggested activation of signal transduction pathways, including *TLR8*, *IL10RB*, and *IL16*. In contrast, clusters 3 and 5 contained genes downregulated in all treatment conditions, with the combination inducing a markedly more pronounced effect over single agents, particularly in cluster 5 (Figure 1G-H). This cluster comprised genes associated with proliferation and apoptosis (*FLT3*, *MEF2C*, *BCL2*) as well as with development (supplemental Tables 2 and 3), in agreement with the enhanced antiproliferative effect and apoptosis induced by combinatorial treatment. Finally, cluster 2 involved genes differentially changed by single agents: upregulated by gilteritinib and downregulated by MI-3454, but demonstrating even stronger downregulation by combinatorial treatment. This cluster included genes critical for leukemogenesis, such as *MEIS1*, *HOXA3*, *HOXA7*, *HOXA11*, and *RUNX2* (Figure 1G-H; supplemental Tables 2 and 3), providing evidence of an enhanced antileukemic effect of the combination. Gene set enrichment analysis revealed that the combination of gilteritinib and MI-3454 strongly affected many gene programs, including those related to loss of stemness and induction of differentiation as well as suppression of oncogenic *MYC* pathways (Figure 1I-J; supplemental Figure 5B; supplemental Table 4), further rationalizing the enhanced antileukemic effect observed with the combination.

We then assessed the in vivo effect of combining menin and FLT3 inhibitors. First, we used the aggressive MOLM13 xenotransplantation model and found that both single-agent (MI-3454 and AC-220) and combinatorial treatment blocked leukemia progression during the treatment period, reflected by a very low level of leukemic blasts (human $CD45^+$ [$hCD45^+$]) in peripheral blood (PB; Figure 2A; supplemental Figure 6A-C). However, once the treatment was stopped, the single agent–treated mice developed leukemia, resulting in a doubling of survival over vehicle (Figure 2A-B). Remarkably, 6 of 8 mice in the combination group did not show any signs of leukemia and had no measurable disease even 9 months after stopping the treatment (Figure 2B; supplemental Figure 6D**)**. These mice had also small spleens and demonstrated highly differentiating phenotypes of bone marrow cells (Figure 2C-D; supplemental Figure 6E). Importantly, the complete remission observed in this aggressive model of *MLL1*-rearranged leukemia was achieved only in the combination group, with a majority of mice cured of leukemia.

Next, we developed and used a PDX model derived from the AML patient sample harboring MLL-ENL, FLT3 S451, and NRAS mutations (MLL-6315 PDX; supplemental Table 5). Treatment of mice with MI-3454, gilteritinib, or their combination was initiated when the level of $hCD45^+$ cells in PB reached ~2% and was continued for 28 days, resulting in no substantial toxicity (supplemental Figure 7A-B). Interestingly, during the treatment period, the blast level in PB initially increased in all treatment groups (day 8 of treatment), but later, it dropped substantially in MI-3454 and combination groups (Figure 2E). The vehicle- and gilteritnib-treated mice developed terminal leukemia, with no significant difference in survival (Figure 2H; supplemental Figure 7C). Interestingly, despite a strong reduction in the blast level of MI-3454–treated mice (days 8-28 of treatment), these mice eventually developed leukemia, with survival double that of vehicle control (Figure 2E-F,H). Remarkably, complete remission was achieved in the combination group, with no blasts detected in PB even at 7.5 months after completion of treatment, supporting no measurable disease (Figure 2E-H; supplemental Figure 7D), and with all mice cured of leukemia.

To assess whether combinatorial treatment with menin and an FLT3 inhibitor is effective in *NPM1*-mutated leukemia with an FLT3-ITD, we used a PDX model derived from the AML primary sample harboring both mutations (NPM1-5577 PDX; supplemental Table 5). Gilteritinib as a single agent did not show a significant effect on leukemia progression in this PDX model (Figure 2I-J). Interestingly, although MI-3454 was initially very effective in reducing leukemia progression, after 40 days of treatment, the level of $hCD45^+$ cells increased in this group, likely because of the reduced dose (from a twice- to once-daily schedule) administered as a result of limited tolerability in the combination group (Figure 2I-J; supplemental Figure 8A-B). Remarkably, in the combination group, the blast level remained very low (<0.5%) over the entire course of the experiment, demonstrating a superior effect of combination over menin or FLT3 inhibitors in the *NPM1*-mutated leukemia model (Figure 2I-J; supplemental Figure 8C-D).

In summary, our study demonstrates the strong synergistic effect of the combination of menin and FLT3 inhibitors. Although

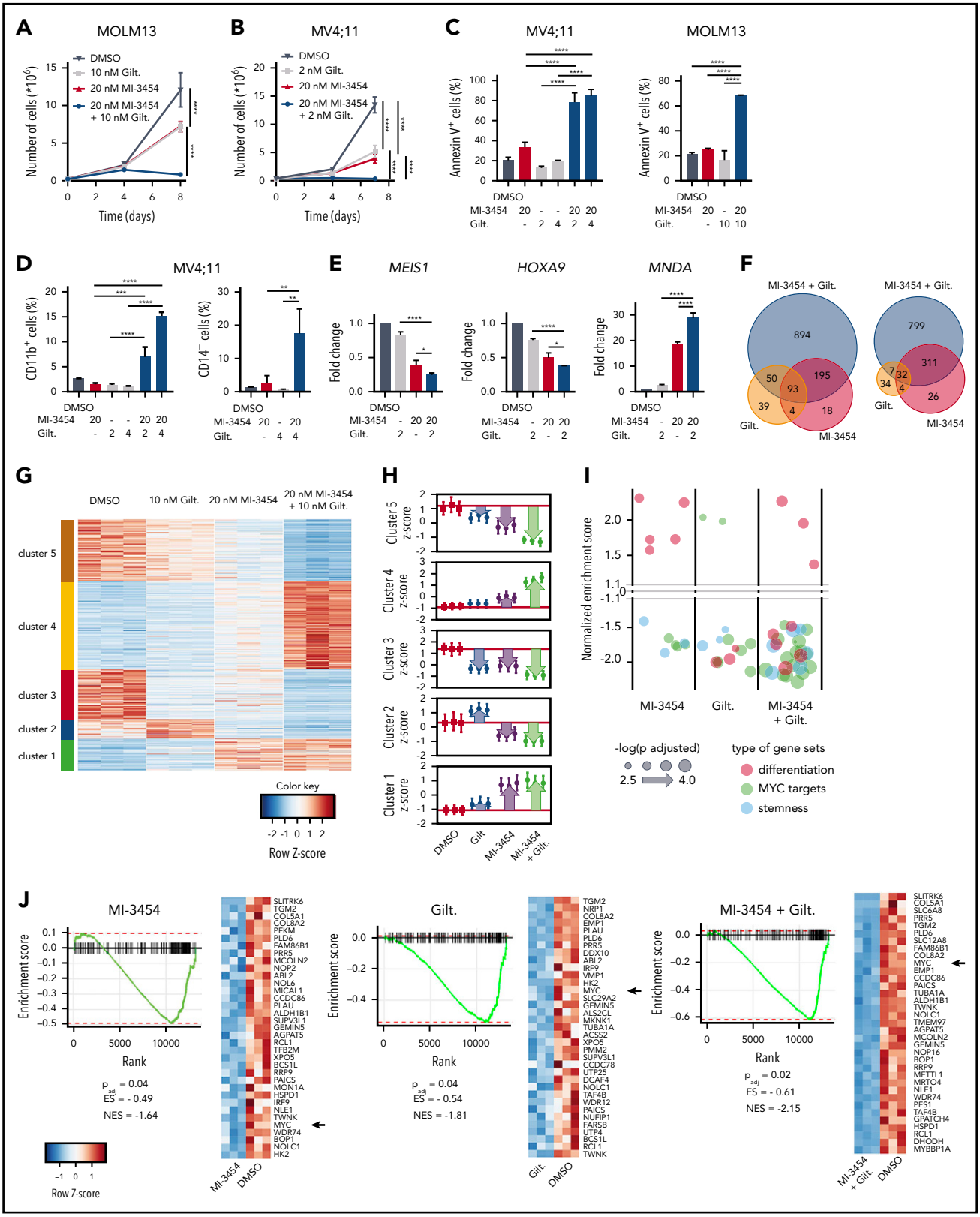

Figure 1. Effect of combinatorial treatment with menin and FLT3 inhibitors in leukemia cells. (A-B) Growth inhibition in MOLM13 (expressing MLL-AF9 and FLT3-ITD) (A) and MV4;11 cells (expressing MLL-AF4 and FLT3-ITD) (B) treated with MI-3454, gilteritinib (Gilt), or their combination. (C) Flow cytometric analysis of apoptosis (annexin V$^+$ cells) induced after 8 days of treatment of MOLM13 and MV4;11 cells with MI-3454, Gilt, or their combination. (D) Flow cytometric quantification of differentiation markers (CD11b$^+$ and CD14$^+$) in MV4;11 cells after single-agent or combinatorial treatment with MI-3454 and Gilt. (E) Gene expression studies in MV4;11 cells after 8 days of treatment with MI-3454, Gilt, or their combination. (A-E) Graphs are representative of 2 independent experiments performed in triplicate. (F-H) Comparison of differentially expressed (DE) genes (adjusted $P < .05$; fold change >|1.5|) from RNA sequencing (RNA-seq) studies in MOLM13 cells after 8 days of treatment with dimethyl sulfoxide (DMSO), MI-3454, Gilt, or their

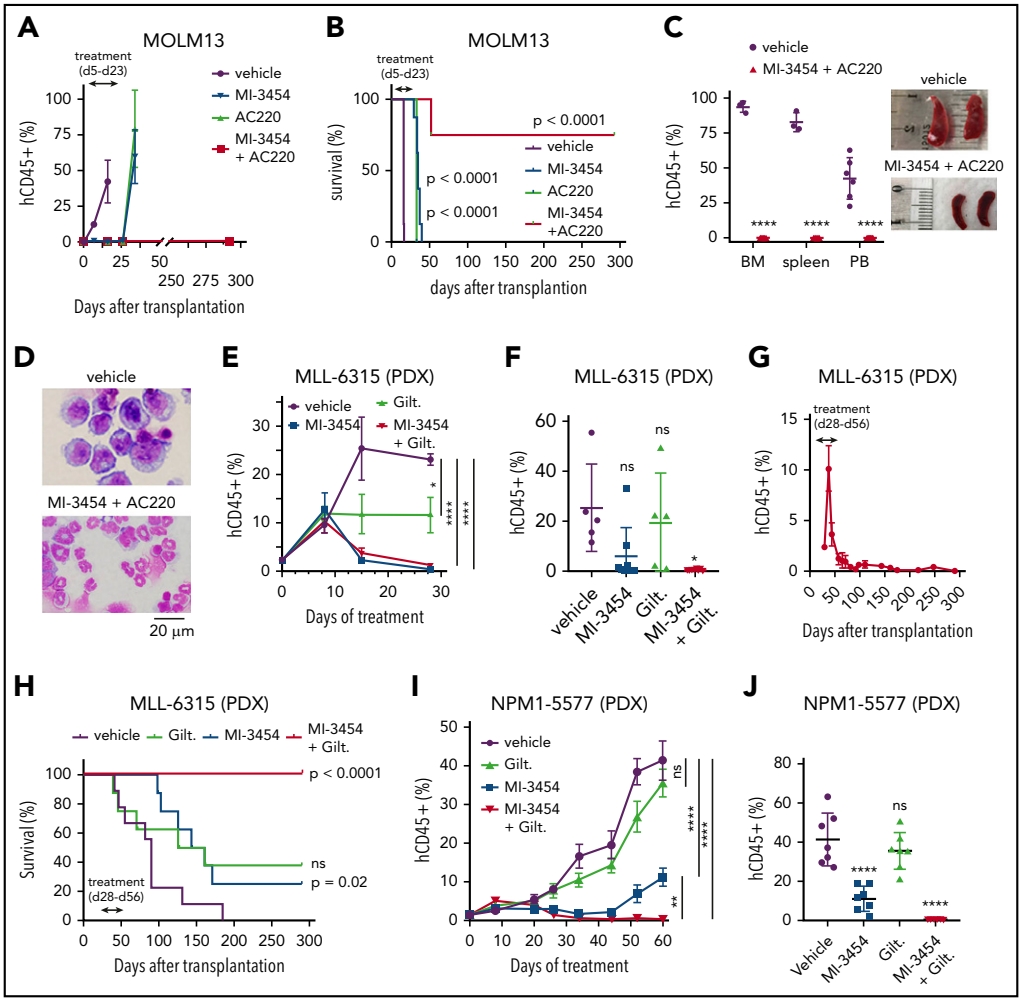

Figure 2. In vivo combinatorial treatment with menin and FLT3 inhibitors. (A) Flow cytometric quantification of hCD45$^+$ cells in PB of mice during treatment with vehicle, MI-3454 (100 mg/kg orally twice daily), AC220 (10 mg/kg orally once daily), or a combination of the 2 agents (doses same as for single agents) in the MOLM13 xenotransplantation model. Mean ± standard error of the mean (SEM; n = 8). (B) Kaplan-Meier survival curves in the MOLM13 xenotransplantation model. Doses as in panel A. *P* values were calculated using log-rank (Mantel-Cox) test. (C) Left: flow cytometric quantification of hCD45$^+$ cells in PB, spleen, and bone marrow (BM) samples harvested from the vehicle-treated mice (at the terminal stage of leukemia: day 16 posttransplantation) and mice treated with the combination of MI-3454 and AC220 (samples collected at day 292 posttransplantation) in the MOLM13 model. Mean ± standard deviation (SD; n = 3-6 [vehicle: n = 6 for PB, n = 3 for BM and spleen; MI-3454 + AC220 group: n = 6). Right: images of spleens collected from the vehicle and combination cohorts of mice. (D) Wright-Giemsa–stained cytospins for BM samples isolated from the vehicle and MI-3454 + AC220 cohorts of MOLM13 mice at the same time points as in panel C. (E) Flow cytometric quantification of hCD45$^+$ cells in PB of MLL-6315 patient-derived xenograft (PDX) mice during treatment with vehicle, MI-3454 (80 mg/kg orally twice daily), gilteritinib (Gilt; 35 mg/kg orally once daily), or the combination of MI-3454 and Gilt (doses same as for single agents). Mean ± SEM (n = 8). (F) Flow cytometric quantification of hCD45$^+$ cells in PB from MLL-6315 PDX mice 27 days after treatment was stopped (day 82 posttransplantation). Doses as in panel E. Mean ± SD. (G) Flow cytometric quantification of hCD45$^+$ cells in PB of MLL-6315 PDX mice treated with the combination of MI-3454 and Gilt. Mean ± SEM (n = 8). (H) Kaplan-Meier survival curves for MLL-6315 PDX mice (n = 8). Treatment doses as in panel E. Treatment time is indicated by the arrow. *P* values were calculated using the log-rank (Mantel-Cox) test. (I) Flow cytometric quantification of hCD45$^+$ cells in PB of NPM1-5577 PDX mice during 60 days of treatment with vehicle, Gilt (35 mg/kg orally once daily), MI-3454 (80 mg/kg twice daily for the first 28 days, followed by 80 mg/kg orally once daily for an additional 32 days; treatment with MI-3454 was reduced to once-daily administration because of limited tolerance of prolonged treatment in the combination group), or combination of MI-3454 and Gilt (doses same as for single agents). Mean ± SD (n = 7). (J) Flow cytometric quantification of hCD45$^+$ cells in PB of NPM1-5577 PDX mice at the last day of treatment. Mean ± SD. *$P < .05$, **$P < .01$, ****$P < .0001$ by 2-tailed Student *t* test (C) or 2- (E,I) or 1-way (F,J) analysis of variance with Tukey multiple comparison test. ns, not significant.

the MI-3454 developed by us as well as the recently published VTP-50469 manifested potent antileukemic activity in *MLL1*-rearranged and *NPM1*-mutated leukemias as single agents, they led to complete remission only in selected leukemia models.[9,10] In this study, we discovered that only the combination of menin and FLT3 inhibitors could cure mice in aggressive

Figure 1 (continued) combination (n = 3 samples per treatment group). (F) Venn diagrams show the overlap of upregulated DE genes (right) and downregulated DE genes (left) relative to DMSO. (G) Heatmap of DE genes after k-means clustering of DE genes using a priori–determined 5 clusters. (H) Average *z* scores for all treatment groups calculated within each k-means cluster. (I) Summary of fast gene set enrichment analysis results for gene sets relating to targets of MYC, differentiation, or stemness from the RNA-seq studies in MOLM13. Each bubble represents a gene set. Size of bubbles on the plot indicates the level of significance, and y-axis indicates the normalized enrichment score (NES) for the gene sets. (J) Representative gene set enrichment plots for MYC targets for each treatment condition relative to DMSO for the Bild_Myc_Oncogenic_Signature gene set from MSigDB. The heatmaps show genes comprising the leading edge of the gene set enrichment plots. Red indicates high expression; blue indicates low expression; black arrows indicate *MYC*. *$P < .05$, **$P < .01$, ***$P < .001$, ****$P < .0001$ by 2- (A-B) or 1-way (C-E) analysis of variance with Tukey multiple comparison test. adj, adjusted; ES, enrichment score.

leukemia models harboring activating FLT3 mutations in addition to *MLL1* translocations or *NPM1* mutations. Mechanistically, this combination induced stronger downregulation of *MEIS1* and *HOXA* cluster genes and demonstrated a more pronounced effect on *MYC*, stemness, and differentiation pathways over single agents, concurring with a recent report.[25] Importantly, we found that the combination of potent menin and FLT3 inhibitors was particularly effective in vivo, leading to complete and long-lasting remission of leukemia in mice. Our findings can be directly translated to initiate clinical trials with this combination in AML patients.

Acknowledgments

The authors thank Martin Carroll from the Stem Cell and Xenograft Core at the University of Pennsylvania for providing patient samples for these studies. The mouse work was performed under the oversight of the University Committee on Use and Care of Animals at the University of Michigan.

This work was supported by Kura Oncology, Inc.; National Institutes of Health (NIH), National Cancer Institute (NCI) R01 grants 1R01CA160467 and 1R01CA201204 (J.G.); NIH, NCI R01 grants 1R01 CA207272 and 1R01 CA226759 (T.C.); a Leukemia & Lymphoma Society (LLS) Scholar Award (1215-14; J.G.); an LLS Scholar Award (T.C.); American Cancer Society Mission Boost grant MBG-19-095-01-COUN (J.G.); and NIH T32 training grant T32DK007519 (J.R.) from National Institute of Diabetes and Digestive and Kidney Diseases.

Authorship

Contribution: S.K. and D.C. designed and synthesized compounds; H.M., K.K., and E.K. designed and performed in vivo efficacy studies and biological studies in leukemia cell lines and primary patient samples; T.P. performed cell biology experiments; G.D.-D. and W.T. supported the project with primary patient samples and interpreted data; J.R. analyzed RNA sequencing data; and J.G. and T.C. directed the entire project, designed the experiments, analyzed the results, and wrote the manuscript, with input from all authors.

Conflict-of-interest disclosure: J.G. and T.C. have received research support from Kura Oncology, Inc.; have served as consultants for Kura Oncology, Inc., and have equity ownership in the company; and are coinventors on patent applications covering MI-3454. S.K. and H.M. are coinventors on patent applications covering MI-3454 or related compounds, which were licensed by Kura Oncology, Inc. J.G., T.C., S.K., and H.M. receive royalties from the University of Michigan on patents covering menin inhibitors, which were licensed to Kura Oncology, Inc. The remaining authors declare no competing financial interests.

ORCID profiles: H.M., 0000-0003-4862-9484; T.P., 0000-0003-0697-4140; J.G., 0000-0002-6180-9095.

Correspondence: Jolanta Grembecka, Department of Pathology, University of Michigan, 1150 West Medical Center Dr, MSRB I, Room 4510D, Ann Arbor, MI, 48108; e-mail: jolantag@umich.edu; or Tomasz Cierpicki, Department of Pathology, University of Michigan, 1150 West Medical Center Dr, MSRB I, Room 4510C, Ann Arbor, MI, 48108; e-mail: tomaszc@umich.edu.

Footnotes

Submitted 22 April 2020; accepted 24 September 2020; prepublished online on *Blood* First Edition 5 October 2020.

*H.M., E.K., D.C., and T.P. contributed equally to this work.

RNA sequencing data for MOLM13 cells treated with dimethyl sulfoxide, MI-3454, gilteritinib, or combination of MI-3454 and gilteritinib were submitted to the Gene Expression Omnibus database (accession code GSE149049).

The online version of this article contains a data supplement.

REFERENCES

1. Yokoyama A, Somervaille TC, Smith KS, Rozenblatt-Rosen O, Meyerson M, Cleary ML. The menin tumor suppressor protein is an essential oncogenic cofactor for MLL-associated leukemogenesis. *Cell*. 2005;123(2):207-218.
2. Yokoyama A, Cleary ML. Menin critically links MLL proteins with LEDGF on cancer-associated target genes. *Cancer Cell*. 2008;14(1):36-46.
3. Kühn MW, Song E, Feng Z, et al. Targeting chromatin regulators inhibits leukemogenic gene expression in NPM1 mutant leukemia. *Cancer Discov*. 2016;6(10):1166-1181.
4. Grembecka J, He S, Shi A, et al. Menin-MLL inhibitors reverse oncogenic activity of MLL fusion proteins in leukemia. *Nat Chem Biol*. 2012;8(3):277-284.
5. Borkin D, He S, Miao H, et al. Pharmacologic inhibition of the menin-MLL interaction blocks progression of MLL leukemia in vivo. *Cancer Cell*. 2015;27(4):589-602.
6. Shi A, Murai MJ, He S, et al. Structural insights into inhibition of the bivalent menin-MLL interaction by small molecules in leukemia. *Blood*. 2012;120(23):4461-4469.
7. He S, Malik B, Borkin D, et al. Menin-MLL inhibitors block oncogenic transformation by MLL-fusion proteins in a fusion partner-independent manner. *Leukemia*. 2016;30(2):508-513.
8. Borkin D, Klossowski S, Pollock J, et al. Complexity of blocking bivalent protein-protein interactions: development of a highly potent inhibitor of the menin-mixed-lineage leukemia interaction. *J Med Chem*. 2018;61(11):4832-4850.
9. Klossowski S, Miao H, Kempinska K, et al. Menin inhibitor MI-3454 induces remission in MLL1-rearranged and NPM1-mutated models of leukemia. *J Clin Invest*. 2020;130(2):981-997.
10. Krivtsov AV, Evans K, Gadrey JY, et al. A menin-MLL inhibitor induces specific chromatin changes and eradicates disease in models of MLL-rearranged leukemia. *Cancer Cell*. 2019;36(6):660-673.e11.
11. Uckelmann HJ, Kim SM, Wong EM, et al. Therapeutic targeting of preleukemia cells in a mouse model of *NPM1* mutant acute myeloid leukemia. *Science*. 2020;367(6477):586-590.
12. Gilliland DG, Griffin JD. The roles of FLT3 in hematopoiesis and leukemia. *Blood*. 2002;100(5):1532-1542.
13. Thiede C, Steudel C, Mohr B, et al. Analysis of FLT3-activating mutations in 979 patients with acute myelogenous leukemia: association with FAB subtypes and identification of subgroups with poor prognosis. *Blood*. 2002;99(12):4326-4335.
14. Daver N, Schlenk RF, Russell NH, Levis MJ. Targeting FLT3 mutations in AML: review of current knowledge and evidence. *Leukemia*. 2019;33(2):299-312.
15. Libura M, Asnafi V, Tu A, et al. FLT3 and MLL intragenic abnormalities in AML reflect a common category of genotoxic stress. *Blood*. 2003;102(6):2198-2204.
16. Tao S, Wang C, Chen Y, et al. Prognosis and outcome of patients with acute myeloid leukemia based on *FLT3-ITD* mutation with or without additional abnormal cytogenetics. *Oncol Lett*. 2019;18(6):6766-6774.
17. Kiyoi H, Kawashima N, Ishikawa Y. FLT3 mutations in acute myeloid leukemia: therapeutic paradigm beyond inhibitor development. *Cancer Sci*. 2020;111(2):312-322.
18. Stam RW, den Boer ML, Schneider P, et al. Targeting FLT3 in primary MLL-gene-rearranged infant acute lymphoblastic leukemia. *Blood*. 2005;106(7):2484-2490.
19. Balgobind BV, Zwaan CM, Pieters R, Van den Heuvel-Eibrink MM. The heterogeneity of pediatric MLL-rearranged acute myeloid leukemia. *Leukemia*. 2011;25(8):1239-1248.
20. Chillón MC, Gómez-Casares MT, López-Jorge CE, et al. Prognostic significance of FLT3 mutational status and expression levels in MLL-AF4+ and

MLL-germline acute lymphoblastic leukemia. *Leukemia*. 2012;26(11): 2360-2366.

21. Armstrong SA, Kung AL, Mabon ME, et al. Inhibition of FLT3 in MLL. Validation of a therapeutic target identified by gene expression based classification. *Cancer Cell*. 2003;3(2): 173-183.

22. Falini B, Mecucci C, Tiacci E, et al; GIMEMA Acute Leukemia Working Party. Cytoplasmic nucleophosmin in acute myelogenous leukemia with a normal karyotype [published correction appears in *N Engl J Med*. 2005;352(7):740]. *N Engl J Med*. 2005;352(3): 254-266.

23. Papaemmanuil E, Gerstung M, Bullinger L, et al. Genomic classification and prognosis in acute myeloid leukemia. *N Engl J Med*. 2016;374(23):2209-2221.

24. Oyelade J, Isewon I, Oladipupo F, et al. Clustering algorithms: their application to gene expression data. *Bioinform Biol Insights*. 2016;10:237-253.

25. Dzama MM, Steiner M, Rausch J, et al. Synergistic targeting of FLT3 mutations in AML via combined menin-MLL and FLT3 inhibition [published online ahead of print 26 June 2020]. *Blood*. doi:10.1182/blood.2020005037.

DOI 10.1182/blood.2020006575